

## Selective Oxo Functionalization of the Uranyl Ion with 3d Metal Cations

Polly L. Arnold,\* Dipti Patel, Alexander J. Blake, Claire Wilson, and Jason B. Love\*

School of Chemistry, University Park, University of Nottingham, Nottingham NG7 2RD, United Kingdom

Received May 24, 2006; E-mail: polly.arnold@nott.ac.uk

The early actinides, namely uranium, neptunium, and plutonium, all form actinyl cations  $[AnO_2]^{n+}$  ( $An = Np, Pu, n = 1$  or  $2$ ;  $An = U, n = 2$ ) in their high oxidation state chemistry,<sup>1</sup> which are generally considered to be thermodynamically and kinetically inert.<sup>2</sup> This is particularly evident for the linear uranyl dication in which the  $U=O$  bonding involves most of the uranium valence orbitals and so results in ligand chemistry only in the equatorial plane and exceedingly unreactive oxo groups.<sup>3</sup> This contrasts sharply with the extensive Lewis base chemistry of transition metal oxo complexes, which can catalyze hydrocarbon oxidation and oxo atom transfer and take part in a variety of cycloaddition reactions.<sup>4</sup>

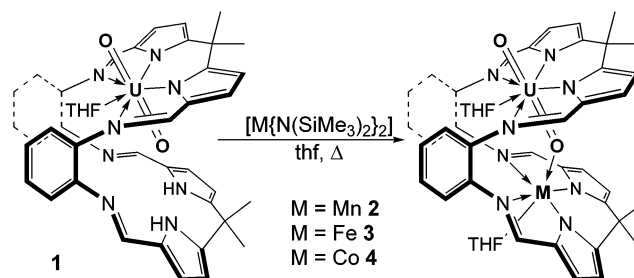
Actinyl complexes that display Lewis base interactions between the oxo and a metal counterion, that is,  $AnO_2^{2+} \cdots M^+$ , so-called cation–cation complexes, are important species in neptunium and plutonium chemistry,<sup>5</sup> but the relative inertness of the uranyl  $AnO_2^{2+}$  moiety means that there are very few simple, molecular uranyl-based cation–cation complexes.<sup>6</sup> Such uranyl analogues would be desirable for understanding the speciation of the highly radioactive metals in nuclear fuel processing and the environment. Of the handful of uranyl cation–cation complexes, which form in the solid state, none are retained in solution. The most notable is the tetrameric  $[UO_2(OCHf-Pr_2)_2]_4$ , the only example in which the solid-state Raman spectrum evidences a significant weakening of the  $UO_2$  bonding.<sup>7</sup> The others are alkali metal adducts such as  $[Na(thf)_2][UO_2\{N(SiMe_3)_2\}_3]$ .<sup>8</sup> One nonmetal, Lewis-acid-functionalized uranyl complex exists, the neutral arylborane adduct  $[UO_2\{B(C_6F_5)_3\}\{PhC(NSiMe_3)_2\}_2]$ , **A**, and is a discrete molecular complex that is the only molecule shown to date to retain uranyl Lewis base behavior in solution.<sup>9</sup>

We have shown recently that the potentially tetra-anionic pyrrole–imine macrocycle, **H<sub>4</sub>**L, forms exclusively the monouranyl adduct  $[UO_2(thf)(H_2L)]$  **1**, Scheme 1. The aryl groups in the macrocycle function as hinges that result in a rigid molecular cleft structure (often called a Pacman structure) in which one uranyl oxo is hydrogen-bonded within the cleft to the pyrrolic hydrogens of the vacant  $N_4$  donor compartment.<sup>10</sup> Herein, we exploit this oxo-group desymmetrization in the synthesis of transition metal adducts of **1** that display the first cation–cation interactions between the uranyl group and a transition metal.

The transamination reaction between the khaki-green uranyl complex  $[UO_2(thf)(H_2L)]$  **1** and  $[M\{N(SiMe_3)_2\}_2]$  in boiling thf affords a brown solution, that, on slow cooling, results in brown crystals of  $[UO_2(thf)M(thf)(L)]$  **2** (Scheme 1). The analogous reaction between **1** and  $[Fe\{N(SiMe_3)_2\}_2]$  or  $[Co\{N(SiMe_3)_2\}_2]$  in thf affords brown  $[UO_2(thf)Fe(thf)(L)]$  **3**, and  $[UO_2(thf)Co(thf)(L)]$  **4**, respectively. Both **2** and **4** were analyzed by single-crystal X-ray diffraction; unfortunately, crystals of **3** were only weakly diffracting. All three heterobimetallic complexes are isolated in yields of 30–40%,<sup>11</sup> show very similar physicochemical behavior, and have been fully characterized, see Supporting Information.

Importantly, the complexes are neutral and undergo neither metal exchange nor redistribution reactions in solution and may be

**Scheme 1.** Synthesis of the Uranyl–Transition Metal Complexes **2**, **3**, and **4**



recrystallized intact from polar, aprotic solvents. In the electrospray mass spectrum of **2** in thf, a peak due to  $[2 + Na]^+$  appears at  $m/z = 1092$  amu. The single-crystal X-ray diffraction data for **2** and **4**, Figure 1, show that the complexes are isostructural and demonstrate interaction between the uranyl oxo atom and a transition metal for the first time. The most striking feature of the structure is the transition metal to uranyl–oxygen bond that is formed within the cavity (designated *endo*). For manganese, **2**, this  $Mn1-O1$  distance is 2.163(4) Å, while the  $U=O1$  bond is correspondingly lengthened to 1.808(4) Å from 1.790(4) Å in **1**. There are no other transition metal–oxo–uranyl complexes reported with which to compare this bond distance, although in the polyoxometalate adduct of octahedral  $Mn^{2+}$ ,  $[n-Bu_4N]_4[Mn(OH)_2\{(\mu-O)_2Mo_5O_{14}(OMe)_2\}_2\{Mn(CO)_3\}_2]$  the four  $Mn-oxo$  distances range between 2.13(2) and 2.18(2) Å.<sup>12</sup>

The resulting desymmetrization of the uranyl cation is shown by the significant difference in **2** (according to the  $3\sigma$  criterion) between the *endo*  $U1-O1$  of 1.808(4) and shorter *exo*  $U1-O2$  distance of 1.768(5), Table 1; the  $U1-O2$  distance is at the short end of the normal  $U=O$  range.<sup>1</sup>

The manganese ion adopts a pseudo-tetrahedral geometry and is coordinated by both pyrrolic nitrogens, the *endo* uranyl oxo in the cavity, and a molecule of thf opposite to the *endo* oxo; only weak interactions to the two imino N atoms occur ( $Mn1-N5$ , 2.547(5);  $Mn1-N8$ , 2.659 Å), presumably as a consequence of the  $\pi$ -stacked thf on the uranyl ion causing the aryl hinge to “open”. The equatorial ligand set in the uranyl half of the complex in **2** remains relatively similar to that of **1**, in which the thf molecule occupied an unusual and unfavorable  $\pi$ -stacking position between the two hinge arenes. Unlike in **1**, however, the thf molecule bound to  $U1$  in **2** is distorted out of the  $UN_4$  equatorial plane ( $O3$  0.3 Å o.o.p.). This distortion is favorable in  $\pi$ -stacking terms but unfavorable in terms of the equatorial bonding preference for uranyl ligands and may be a combined consequence of the proximate thf bound to the manganese and the rigid cleft structure.

The  $U-N$  and  $Mn-N$  imino and pyrrolic distances are normal for  $U^{VI}$  and  $Mn^{II}$ <sup>13</sup> and so suggest that the metal oxidation states are unchanged in the formation of **2**. This is reinforced by magnetic susceptibility measurements for **2**, **3**, and **4**, which have been studied in the solid state by SQUID magnetometry over the temperature range 2–300K. The moments at 300K and 80K are collated in Table

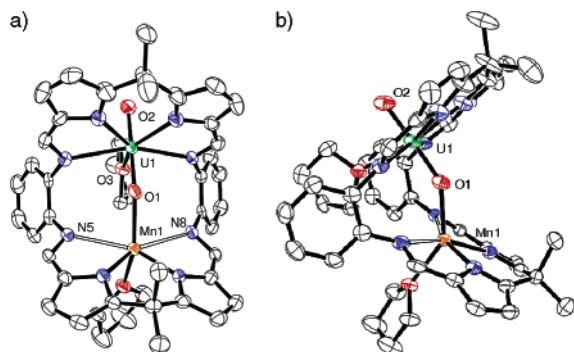


**Figure 1.** Displacement ellipsoid drawing of **2** (isostructural with **4**) with 50% probability ellipsoids. (a) Front view and (b) side view. Hydrogen atoms and lattice solvent molecules are omitted for clarity. Selected distances (Å) are in Table 1.

**Table 1.** Comparison of Selected Single Crystal Diffraction, Spectroscopic, and Magnetic Data for Complexes **1–4**

no.	M	bond lengths (Å) <sup>a</sup>			$\nu_{\text{UO}_2}$ <sup>b</sup> (cm <sup>-1</sup> )	$\mu_{\text{eff}}^c$ ( $\mu_B$ )	
		U–O2	U–O1	M–O1	Raman	80 K	300 K
<b>1</b>		1.766(4)	1.790(4)		817		
<b>2</b>	Mn	1.768(5)	1.808(4)	2.163(4)	811	5.25	5.40
<b>3</b>	Fe				804	4.99	5.24
<b>4</b>	Co	1.771(6)	1.784(6)	2.084(6)	807	4.10	4.27

<sup>a</sup> Single-crystal X-ray diffraction data. <sup>b</sup> Uranyl stretch. <sup>c</sup> SQUID magnetometer.

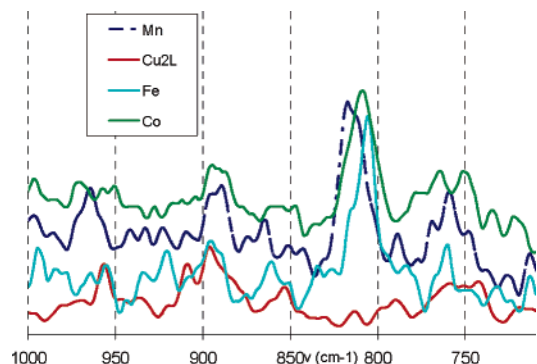


**Figure 2.** Raman spectra for the complexes **2** to **4** in the fingerprint region Mn = **2**, Fe = **3**, and Co = **4**.

1. The data for all three are fitted very well by models that assume  $\text{U}^{\text{VI}}\text{M}^{\text{II}}$  oxidation states with high-spin configurations for the transition metal cations and Curie–Weiss paramagnetic behavior. This oxidation state agrees with the crystallographically determined structures and also the inertness of the uranyl  $\text{U}^{\text{VI}}$  to reduction.

Vibrational spectroscopy should also indicate the strength of the uranyl bonding.<sup>14</sup> The lowered symmetry due to transition metal coordination should afford two IR and Raman active uranyl stretches in the region around 800–900  $\text{cm}^{-1}$ . Figure 2 contains the solid-state Raman spectra of the complexes in this region.

The IR and Raman spectra of **2** to **4** are complicated by overlapping ligand absorptions (see SI for the IR spectra of **2–4**, including two nonuranyl containing, Pacman-shaped complexes,  $\text{Cu}_2\text{L}$  and  $\text{Pd}_2\text{L}$ ,<sup>15</sup> for comparison). However, the absorption in each complex at 811  $\text{cm}^{-1}$  (**2**), 804  $\text{cm}^{-1}$  (**3**), and 807  $\text{cm}^{-1}$  (**4**), observed in the Raman spectrum, is absent in the similarly Pacman-shaped complex,  $\text{Cu}_2\text{L}$ , see Figure 2. Therefore, we can assign this absorption to the uranyl unit. The simplest, symmetrical  $[\text{UO}_2]^{2+}$  cation  $[\text{UO}_2(\text{OH}_2)_5]^{2+}$  has a symmetric  $\nu_1$  stretch at 870  $\text{cm}^{-1}$  in the Raman spectrum;<sup>16</sup> the  $\nu_1$  stretch for  $[\text{Na}(\text{thf})_2][\text{UO}_2\{\text{N}(\text{SiMe}_3)_2\}_3]$  is 805  $\text{cm}^{-1}$  and that for **A** at 785  $\text{cm}^{-1}$ .

In conclusion, these complexes are the first molecular transition metal uranyl adducts, that is, cation–cation complexes between transition metals and the uranyl cation, and also the first uranyl-metal complexes that retain their integrity in solution. The  $\text{Mn}^{\text{II}}$  complex **2** exhibits a significant lengthening of the *endo* uranyl oxo bond, and the corresponding  $\text{UO}_2$  stretching vibrations are weakened. Significantly, the transition metal cations presented in this study are common in both minerals and uranium wastes, and iron is often implicated in uranyl reduction chemistry in vitrified materials and geological samples.<sup>17</sup>

We hope that these molecular cation–cation complexes will allow access to the selective chemical reactivity of one uranyl oxygen.

**Acknowledgment.** We thank the EPSRC and the Royal Society for funding and Dr Stephanie M. Cornet of the University of Manchester for assistance with the Raman spectroscopy.

**Supporting Information Available:** Synthetic, crystallographic, and spectroscopic data for all bimetallic complexes. This material is available free of charge via the Internet at <http://pubs.acs.org>.

## References

- (1) (a) Katz, J. J.; Morss, L. R.; Seaborg, G. T. *Summary and Comparative Aspects of the Actinide Elements*; Chapman & Hall: London, 1986. (b) Wilson, P. D. In *The Nuclear Fuel Cycle*; Wilson, P. D., Ed.; OU Press: Oxford, U.K., 1996.
- (2) (a) Sessler, J. L.; Melfi, P. J.; Pantos, G. D. *Coord. Chem. Rev.* **2006**, *250*, 816. (b) Denning, R. G.; Green, J. C.; Hutchings, T. E.; Dallera, C.; Tagliaferri, A.; Giarda, K.; Brookes, N. B.; Braicovich, L. *J. Chem. Phys.* **2002**, *117*, 8008.
- (3) (a) King, R. B. *J. Coord. Chem.* **2005**, *58*, 47. (b) Szabo, Z.; Toraiishi, T.; Vallet, V.; Grenthe, I. *Coord. Chem. Rev.* **2006**, *250*, 784.
- (4) Nugent, W. A.; Mayer, J. M. *Metal–Ligand Multiple Bonds*; Wiley: New York, 1988.
- (5) (a) Reilly, S. D.; Neu, M. P. *Inorg. Chem.* **2006**, *45*, 1839. (b) Sessler, J. L.; Gorden, A. E. V.; Seidel, D.; Hannah, S.; Lynch, V.; Gordon, P. L.; Donohoe, R. J.; Tait, C. D.; Keogh, D. W. *Inorg. Chim. Acta* **2002**, *341*, 54. (c) Gorden, A. E. V.; Xu, J. D.; Raymond, K. N.; Durbin, P. *Chem. Rev.* **2003**, *103*, 4207.
- (6) John, G. H.; May, I.; Sarsfield, M. J.; Steele, H. M.; Collison, D.; Helliwell, M.; McKinney, J. D. *Dalton Trans.* **2004**, 734.
- (7) Wilkerson, M. P.; Burns, C. J.; Dewey, H. J.; Martin, J. M.; Morris, D. E.; Paine, R. T.; Scott, B. L. *Inorg. Chem.* **2000**, *39*, 5277.
- (8) (a) Burns, C. J.; Clark, D. L.; Donohoe, R. J.; Duval, P. B.; Scott, B. L.; Tait, C. D. *Inorg. Chem.* **2000**, *39*, 5464. (b) Danis, J. A.; Lin, M. R.; Scott, B. L.; Eichhorn, B. W.; Runde, W. H. *Inorg. Chem.* **2001**, *40*, 3389. (c) Sarsfield, M. J.; Helliwell, M.; Raftery, J. *Inorg. Chem.* **2004**, *43*, 3170. (d) Benetollo, G.; Bombieri, G.; Herrero, P.; Rojas, R. M. *J. Alloys Compd.* **1995**, *225*, 400. (e) Thuery, P. *Chem. Commun.* **2006**, 853.
- (9) Sarsfield, M. J.; Helliwell, M. *J. Am. Chem. Soc.* **2004**, *126*, 1036.
- (10) (a) Arnold, P. L.; Blake, A. J.; Wilson, C.; Love, J. B. *Inorg. Chem.* **2004**, *43*, 8206. (b) For ligands designed to form hydrogen bonds with uranyl oxo groups, see: Franczyk, T. S.; Czerwinski, K. R.; Raymond, K. N. *J. Am. Chem. Soc.* **1992**, *114*, 8138.
- (11) Analysis of the remaining material after isolation of the second crop of **2** suggests it is the same material, but we did not collect further crops.
- (12) Villanneau, R.; Proust, A.; Robert, F.; Gouzerh, P. *Chem.–Eur. J.* **2003**, *9*, 1982.
- (13) (a) Reid, S. D.; Blake, A. J.; Wilson, C.; Love, J. B. *Inorg. Chem.* **2006**, *45*, 636. (b) Sessler, J. L.; Mody, T. D.; Dulay, M. T.; Espinoza, R.; Lynch, V. *Inorg. Chim. Acta* **1996**, *246*, 23.
- (14) Allen, P. G.; Bucher, J. J.; Clark, D. L.; Edelstein, N. M.; Ekberg, S. A.; Gohdes, J. W.; Hudson, E. A.; Kaltsoyannis, N.; Lukens, W. W.; Neu, M. P.; Palmer, P. D.; Reich, T.; Shuh, D. K.; Tait, C. D.; Zwick, B. D. *Inorg. Chem.* **1995**, *34*, 4797.
- (15) (a) Givaja, G.; Blake, A. J.; Wilson, C.; Schröder, M.; Love, J. B. *Chem. Commun.* **2003**, 2508. (b) Givaja, G.; Schröder, M.; Love, J. B. Unpublished results, 2006.
- (16) Nguyen-Trung, C.; Begun, G. M.; Palmer, D. A. *Inorg. Chem.* **1992**, *31*, 5280.
- (17) (a) Scott, T. B.; Allen, G. C.; Heard, P. J.; Randell, M. G. *Geochim. Cosmochim. Acta* **2005**, *69*, 5639. (b) Zhong, L. R.; Liu, C. X.; Zachara, J. M.; Kennedy, D. W.; Szecsody, J. E.; Wood, B. J. *Environ. Qual.* **2005**, *34*, 1763.

JA0634167